Proceedings of the XII International Symposium on Dynamic Problems of Mechanics (DINAME 2007),
Varoto, P. S. and Trindade, M. A. (Editors), ABCM, Ilhabela, SP, Brazil, February 26 - March 2, 2007

Aeroelastic Analysis of Non-linear Airfoil

Carlos De Marqui Junior [1], Paulo R. Caixeta Junior [2], and Thiago R. Cicogna [3]

[1, 2] University of Sao Paulo, Engineering School of Sao Carlos, Lab. of Aeroelasticity

demarqui@sc.usp.br, caixeta@sc.usp.br

[3] University of Sao Paulo, Engineering School of Sao Carlos, Lab. of Dynamics

thcic@sc.usp.br

Abstract: A variety of non-linear effects can degrade the aeroelastic behavior of typical aeronautical structures, leading to adverse instabilities. Compressibility and separated flows effects are important aspects that result in non-linear aerodynamic behavior, nonetheless, their modeling still a considerable challenge. In terms of structural dynamics the effect of aging, loose attachments, worn of hinges of control surfaces and certain material features are examples of non-linearities to be considered. More recently, the combination of aero-structural non-linear effects has been of great interest for aeroelasticity. In order to study non-linear aeroelastic responses, this work proposes a 3D aeroelastic model based on linear aerodynamics and concentrated structural non-linearities. A typical section with a hinged control surface is considered and the hinge stiffness of the control surface is assumed to be non-linear. Several combinations of non-linearities for the airfoil and control surface stiffnesses can be considered. A combined non-linearity is adopted for the control surface hinge stiffness. The authors intend to investigate how the LCOs and chaotic behavior are influenced by the non-linear structural parameters and aeroelastic coupling.

Keywords: aeroelasticity, non-linear behavior, free-play

NOMENCLATURE

a = location of the elastic axis
A = influence coefficients
b = airfoil semichord
c = location of control surface hinge
$f(\alpha)$ = non-linear structural moment
I = mass moment of inertia about elastic axis
k = structural stiffness
L = aerodynamic lift, N
M = aerodynamic moment, Nm
m = mass of the airfoil
n = normal vector
N = number of panels
PTOS = position of collocation points of the panels
r = radius of gyration
RHS = right hand side
S = static mass moment
t = time
w = vertical displacement, m
U = velocity
W = induced velocity
p = pressure, N/m^2

Greek Symbols

α = pitch rotation angle
β = control surface angle
α = angle between two adjacent pins in the same cross-section
η = surface shape
Γ = vortex strength
Δt = time increment
ρ = density
ϕ = velocity potential
ω = uncoupled natural frequencies

Subscripts

α relative to pitch
β relative to control surface
w relative to plunge
i,j relative to panel
f relative to the free-play
∞ relative to freestream

INTRODUCTION

In some aeroelastic analyses linear aerodynamics and structures are assumed and the problem is reduced to the solution of a set of linear equations. The results obtained are quite accurate for a specific range of velocities and structural conditions. However, aerospace systems are inherently non-linear (Dowell, 1995). The presence of these nonlinearities will modify the behavior of the system, neglecting some results obtained from the linear approach. For example, it is shown that the classical linear flutter behavior at a critical velocity can be converted into a periodic or chaotic motion when the non-linear analysis is assumed, i.e. the short term damages of the linear flutter are converted into long term non-linear effects. So, it is important to understand the non-linear aeroelastic responses when designing a flight vehicle (Lee and Kim, 1995).

The presence of nonlinearities in aeroelastic analysis can be divided into aerodynamic and structural properties. A nonlinear aeroelastic system can have both non-linear properties simultaneously or only one of these properties at a time. Compressibility, separated flows, aerodynamic heating and turbulence effects are important aspects that result in non-linear aerodynamic behavior; nonetheless, their modeling still is a considerable challenge and will not be treated in this paper. Lee, Price and Wong (1999) show a comprehensive study of the different types of aerodynamic nonlinearities present on aeroelastic systems.

In terms of structural properties the effect of aging, loose attachments, certain material features, large motions or deformations are examples of non-linearities to be considered. Structural non-linearities can be subdivided into distributed and concentrated ones. Distributed non-linearities are spread over the entire structure representing the

characteristic of materials and large motions, for example (Patil and Hodges, 2004; Brown, 2003). Concentrated non-linearities act locally, representing loose of attachments, worn hinges of control surfaces, aging, and presence of external stores (Lee, Price and Wong, 1999; O'Neil and Strganac, 1998; Bae, Inman and Lee, 2004; Conner et al, 1997; Tang and Dowell, 2006). The concentrated non-linearities can usually be approximated by one of the classical structural non-linearities, namely, cubic, free-play and hysteresis, or by a combination of these, for example, a free-play and a cubic one.

In general a non-linear aeroelastic system has four types of responses, i.e., flutter, divergence, limit cycle oscillation (LCO) and chaotic motion (Lee and Kim, 1995). Flutter is an unstable motion with increasing amplitude at specific velocities and frequencies. Divergence is a static aeroelastic phenomenon. The LCO is a periodic oscillation consisting of a limited number of frequencies and amplitudes. The chaotic motion is a nonperiodic oscillation consisting of a multitude of frequencies and amplitudes. In some cases the LCO and the chaotic motion can occur at a flow speed lower than the linear flutter speed, showing the importance of the non-linear assumption in aeroelastic analyses.

Many authors have examined the non-linear aeroelastic behavior. Freeplay, hysteresis, and cubic stiffness nonlinearities are examined by Woolston, Runyan and Andrews (1957). These authors studied a 2DOF typical section using Wagner's indicial function to represent the linear aerodynamics. It is shown that flutter velocity can be reduced by an increase in initial displacements when freeplay and hysteresis cases are considered in the airfoil rotation. They also found limit cycle oscillations (LCOs) bellow the linear flutter boundary when cubic hardening cases are considered. Price et al (1994) investigated free-play nonlinearities for the torsion mode and found LCOs regions below the linear flutter velocity. Free-play non-linearity for the torsion mode considering linear and non-linear aerodynamic models is also investigated by Tang and Dowell (1993). Zhao and Yang (1990) examined LCOs responses when cubic non-linearities are present in torsion mode of an airfoil subjected to incompressible flow. The linear aerodynamics was modeled using the Theodore function, what is valid when harmonic motion is assumed. Zhao and Hu (2004) performed some aeroelastic analysis of a two-dimensional airfoil section with combined non-linearity of freeplay and cubic stiffening in torsion. They assumed a linear aerodynamic model using an unsteady lumped vortex method. Several authors have also developed control strategies to suppress the long term damages associated with the non-linear aeroelastic behavior (Block and Strganac, 1998; Singh and Yim, 2003; Zhang and Singh, 2001).

This paper presents the study of a non-linear aeroelastic airfoil with a trailing edge control surface. The linear aerodynamic model is accomplished using unsteady lumped vortex method (Katz and Plotkin, 2001). The non-linear structural behavior is obtained assuming a combined nonlinearity in the structural stiffness of the control surface. This nonlinearity can be understood as a combination of a free-play and a cubic stiffening, with a smooth transition between the zones. The aeroelastic responses are obtained via numerical solution of the equations of motion at each time step using a forth order Runge-Kutta method. The investigation of the non-linear responses is performed for different ratios of free-play gap to initial control surface angle.

Non-linear Aeroelastic Model

A two-dimensional airfoil having three degree of freedom, as depicted in Fig. 1, is investigated.

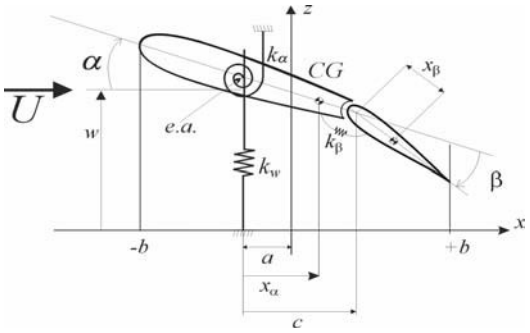

Figure 1 - Structural representation of the aeroelastic model.

The bending and torsion variables are denoted as w and α, respectively, and the control surface motion denoted by β. The bending deflection w is measured at the elastic axis, positive in the upward direction, the torsion angle α is measured at the elastic axis, positive in the nose-up rotation from the *x-axis*, and the control surface angle β is measured at the hinge line, positive in clockwise direction. In addition, ab represents the distance from the elastic axis to midchord, where a is the dimensionless distance between the elastic axis and the midchord, c represents the distance from the elastic axis to control surface hinge axis, b is the semichord of the entire airfoil section. The mass center of the entire airfoil section is located at a distance x_α from the elastic axis and the mass center of the control surface is located at a distance x_β from the hinge line, k_w represents the bending stiffness, k_α the stiffness of the torsion spring, k_β the stiffness of the control surface hinge and U the freestream velocity.

By using Lagrange's equation, the equations of motion of this typical section are obtained. For details the reader can refer to technical literature (Fung, 1993). Here, the dimensionless form of the equation is expressed as,

$$\begin{bmatrix} 1 & -x_\alpha & -x_\beta \\ -x_\alpha & r_\alpha^2 & r_\beta^2 + x_\beta(c-a) \\ -x_\beta & r_\beta^2 + x_\beta(c-a) & r_\beta^2 \end{bmatrix} \begin{bmatrix} \ddot{w} \\ \ddot{\alpha} \\ \ddot{\beta} \end{bmatrix} + \begin{bmatrix} \omega_w^2 & 0 & 0 \\ 0 & r_\alpha^2\omega_\alpha^2 & 0 \\ 0 & 0 & r_\beta^2\omega_\beta^2 \end{bmatrix} \begin{bmatrix} w \\ \alpha \\ \beta \end{bmatrix} = \frac{1}{mb^2} \begin{bmatrix} Lb \\ M_\alpha \\ M_\beta \end{bmatrix} \tag{1}$$

where $x_\alpha = S_\alpha / mb$; $x_\beta = S_\beta / mb$; $\omega_w^2 = k_w / m$; $\omega_\alpha^2 = k_\alpha / I_\alpha$; $\omega_\beta^2 = k_\beta / I_\beta$; $r_\alpha^2 = I_\alpha / mb^2$; $r_\beta^2 = I_\beta / mb^2$

where m the mass of the entire system; I_α is the airfoil mass moment of inertia about the elastic axis; I_β is the control surface mass moment of inertia about the elastic axis; L and M_α are the aerodynamic lift and moment measured about the elastic axis and M_β is the aerodynamic moment on the flap about the flap hinge; S_α and S_β are the static mass moment and ω_w, ω_α and ω_β are the uncoupled natural frequencies.

Non-linear effects due to aerodynamics, damping or structural dynamics can be incorporated to this model. In this work, the structural damping effects are neglected and the source of non-linearities is assumed to be the flap spring, resulting in a non-linear torque. So, when the combined nonlinearity is considered, the non-linear restoring moment about the hinge point can be represented mathematically by,

$$\begin{aligned} f(\beta) &= k_{n\beta}(\beta - \beta_f)^3, \qquad \beta > \beta_f \\ f(\beta) &= 0 \qquad\qquad\quad -\beta_f < \beta < +\beta_f \\ f(\beta) &= k_{n\beta}(\beta + \beta_f)^3, \qquad \beta < -\beta_f \end{aligned} \tag{2}$$

where β_f is the freeplay amplitude and $K_{n\beta}$ is the nonlinear stiffness of the control surface hinge. Figure 2 illustrates this typical concentrated non-linearity in terms of the flap displacement versus torque.

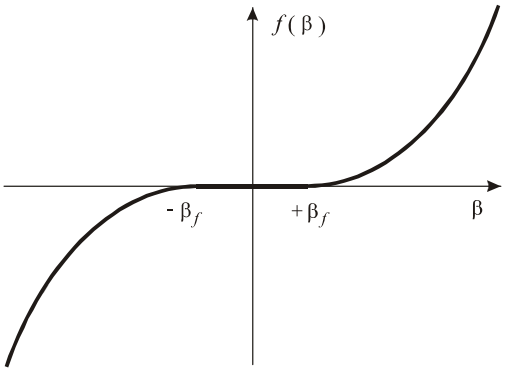

Figure 2. Nonlinear moment when a combined nonlinearity is considered.

The solution of this aeroelastic problem is strictly dependent of the aerodynamic model used to determine the unsteady aerodynamic loads L, M_α and M_β on the right side of Eq. (1). The incompressible potential flow is assumed and the unsteady air loading over the airfoil is solved with the lumped vortex method (Katz and Plotkin, 2001). The thin-airfoil camberline is divided into N panels of the same length. A discrete vortex element is placed at the quarter chord of each panel, this point is called point vortex, and the boundary conditions are observed at the three-quarter chord point, called collocation point. The method is appropriate for the calculation of the unsteady air loading on the airfoil with variable geometry, with the presence of a movable control surface for example, but it is computationally more demanding if compared with that for the rigid airfoil case. Within every time step a new position of point vortices and collocation points of the control surface must be evaluated.

A lumped vortex model for a typical section is shown if Fig. 3. As the airfoil's circulation changes continuously, then a continuous vortex sheet will be shed at the trailing edge, respecting Kelvin's condition. This continuous vortex sheet is approximated by a discrete-vortex wake model, whose vortex elements, Γ_W, are shed at the trailing edge. Two boundary conditions are defined: the zero normal velocity across de body's solid boundaries and the flow disturbance, due to body motion through the fluid, should diminish far away from the body. Moreover, Kelvin and Kutta conditions have to be respected.

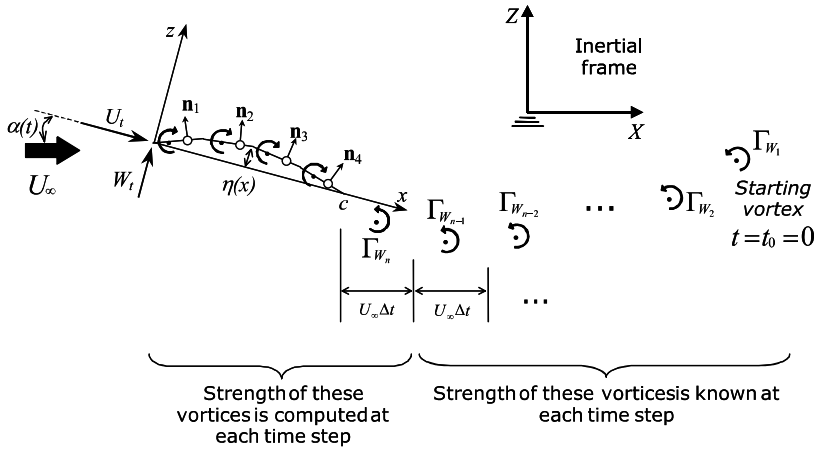

Figure 3. Discrete vortex model for the unsteady air loading calculation on the airfoil (Katz and Plotkin, 2001).

The induced velocities, U_t and W_t, at an arbitrary point (x, z) due to a vortex element Γ_j located at (x_j, z_j) is given by

$$\begin{Bmatrix} U_t \\ W_t \end{Bmatrix} = \frac{\Gamma_j}{2\pi\, r_j^2} \begin{bmatrix} 0 & 1 \\ -1 & 0 \end{bmatrix} \begin{Bmatrix} x - x_j \\ z - z_j \end{Bmatrix} \tag{4}$$

where $r_j^2 = (x - x_j)^2 + (z - z_j)^2$ is the distance between the vortex element and the arbitrary point.

Considering the airfoil camberline divided into N panels, there will be N vortex elements at the N vortex points (x_j, z_j) on the camberline. The zero normal flow boundary condition will be fulfilled on the camberline at the collocation point i of each panel. The normal vector $\mathbf{n}_i$ at each of these collocation points is found in the body's frame,

$$\mathbf{n}_i = \frac{(-d\eta/dx, 1)}{\sqrt{(d\eta/dx)^2 + 1}} = (\sin\alpha_i, \cos\alpha_i) \tag{5}$$

where α_i is the angle between panel i and local x axis, positive nose-up and $\eta(x)$ the surface shape. As the airfoil's control surface position changes with time, vortex and collocation points positions will be always modified.

An influence coefficient A_{ij} can be defined as the velocity component induced by the airfoil's or wake's j^{th} unit strength Γ_j, normal to the surface at the collocation point i. So, an algebraic equation can be obtained for each collocation point i relating the influence coefficients the vortex elements, their strength, and the velocities induced by then into this collocation point. When the entire model is considered the set of equations is obtained,

$$\begin{bmatrix} A_{11} & A_{12} & \cdots & A_{1N} & A_{1W} \\ A_{21} & A_{22} & \cdots & A_{2N} & A_{2W} \\ \vdots & \vdots & \ddots & \vdots & \vdots \\ A_{N1} & A_{N2} & \cdots & A_{NN} & A_{NW} \\ 1 & 1 & \cdots & 1 & 1 \end{bmatrix} \begin{Bmatrix} \Gamma_1 \\ \Gamma_2 \\ \vdots \\ \Gamma_N \\ \Gamma_{W_1} \end{Bmatrix} = \begin{Bmatrix} RHS_1 \\ RHS_2 \\ \vdots \\ RHS_N \\ \Gamma(t - \Delta t) \end{Bmatrix} \tag{6}$$

where each line corresponds to one collocation point. Now, the right-hand side (*RHS*) terms are known at each time step and they are composed by the kinematics velocities due to the motion of the airfoil plus the velocity components induced by wake vortices, except the latest one. As the airfoil's control surface position changes with time, the influence coefficient calculation has also to be done at each time step loop. The Kutta condition is not stated explicitly for the lumped vortex method and the Kelvin condition is represented by

$$\Gamma(t) - \Gamma(t - \Delta t) + \Gamma_W = 0 \tag{7}$$

At each time step the strength of each discrete vortex is determined from the solution of the linear system of Eq. 6. The pressures and airloads are then computed by using the unsteady Bernoulli equation shown in Eq. 8. The total lift and moment are obtained by integrating the pressure difference between the camberline upper and lower surfaces along the chordline. At this point, all the terms necessary to the solution of Eq. (1) are known and it will be solved with the Runge-Kutta method.

$$\frac{p_\infty - p}{\rho} = \frac{1}{2}\left[\left(\frac{\partial \phi}{\partial x}\right)^2 + \left(\frac{\partial \phi}{\partial y}\right)^2 + \left(\frac{\partial \phi}{\partial z}\right)^2\right] - \mathbf{v}\cdot\nabla\phi + \frac{\partial \phi}{\partial t} \tag{8}$$

Linear and Non-linear Aeroelastic Analyses

The aeroelastic behavior of the typical section presented in Fig. 1 has been investigated considering a linear model and a non-linear model. The linear analysis is performed with the aeroelastic model of Eq. (1) and the unsteady lumped vortex aerodynamic model. The non-linear model is similar to the linear one, except for the free-play nonlinearity assumed in the hinge of the control surface. As a consequence, the control surface hinge moment will be the non-linear function presented in Eq. (2).

In the non-linear flutter analysis, the responses are sensitive to the initial conditions. So, the effect of the initial conditions and the effect of free-play quantity on the aeroelastic responses are examined. So, a ratio which considers the free-play gap to the initial control surface angle can be used as a parameter to study the non-linear aeroelastic behavior. This ratio has been defined as gap/initial condition ratio, $R = \beta_f / \beta_0$, where β_0 is the initial angular position of the control surface. The initial conditions considered for linear and non-linear analyses are rigid angles of 0.25, 0.5 or 1.0 degree for the control surface position.

In the aeroelastic analyses, the flutter behavior is defined as a self-sustained oscillatory behavior with increasing amplitudes. The LCO is defined as a bounded motions consisting of a limited number of frequencies and amplitudes. The chaotic behavior is a bounded random-like motion with continuous jump behavior.

The parameters used during the simulations are shown in Tab. 1. All of them have already been defined in the previous section.

Table 1 – Parameters used during typical section simulations.

Parameter	Value	Parameter	Value
ω_w (rad/s)	50.0	x_α	0.2
ω_α (rad/s)	100.0	x_β	0.0125
ω_β (rad/s)	300.0	r_α	0.5
a	-0.4	r_β	0.079
c	0.6	μ	40
b (m)	0.3048	ρ (kg/m^3)	1.225

Linear Analysis

The linear condition is obtained when the gap/initial condition ratio is equal to zero ($\beta_f/\beta_0 = 0$), i.e., the free-play gap is zero. Figure 4 shows the time responses for the linear case when the flow velocity of 75 m/s is considered. The responses are damped out as time proceeds, and the system has a stable behavior.

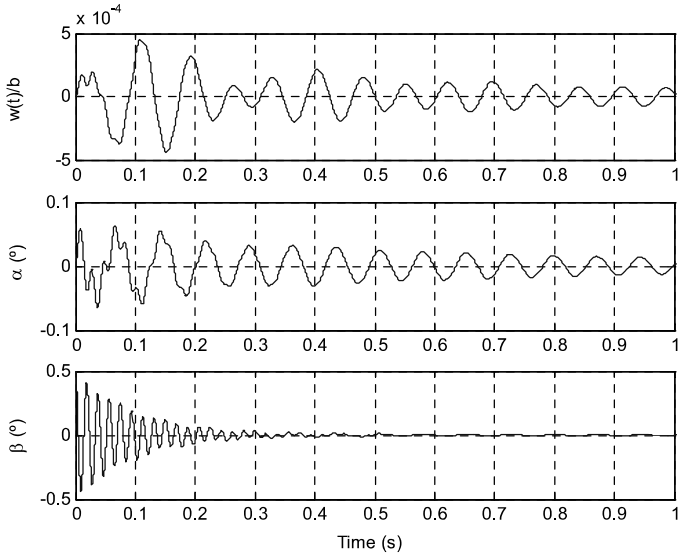

Figure 4. Time responses of the linear model for the velocity of 75 m/s ($R = 0$).

When the flow velocity is 85 m/s the linear aeroelastic system presents the typical flutter behavior. The divergent oscillatory behavior is observed in Fig. 5.

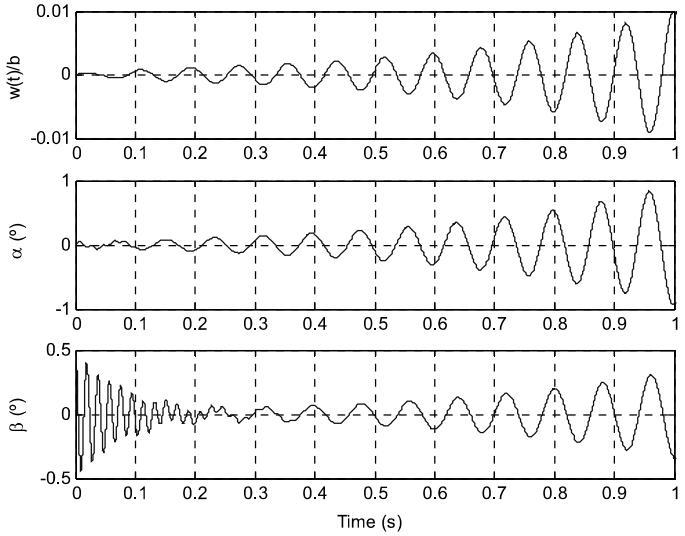

Figura 5. Time responses of the linear model for the velocity of 85 m/s (*R* = 0).

Non-Linear Analysis

The non-linear behavior is obtained when a free-play amplitude of ± 0.5 degrees is considered for the control surface degree of freedom. So the gap/initial condition ratio, *R*, of 2.0, 1.0 and 0.5 are considered when β_0 = 0.25, 0.5, 1.0 degree respectively.

Figure 6 represents the time responses and phase trajectories of the non-linear case (*R* = 2.0, 1.0 and 0.5) for the velocity of 45 m/s. As can be observed, the system is sensitive to the initial conditions. For *R* = 2.0, the continual jump phenomenon is observed. This continual jump has a nonperiodic motion consisting of a multitude of frequencies and amplitudes and is classified as the chaotic motion in this study. This behavior can also be observed in the phase trajectory. For *R* = 1.0 the response is damped out around one of the free-play corners as time proceeds. For *R* = 0.5, the continual jump phenomenon is observed and the chaotic motion around the two corners of the free-play is observed.

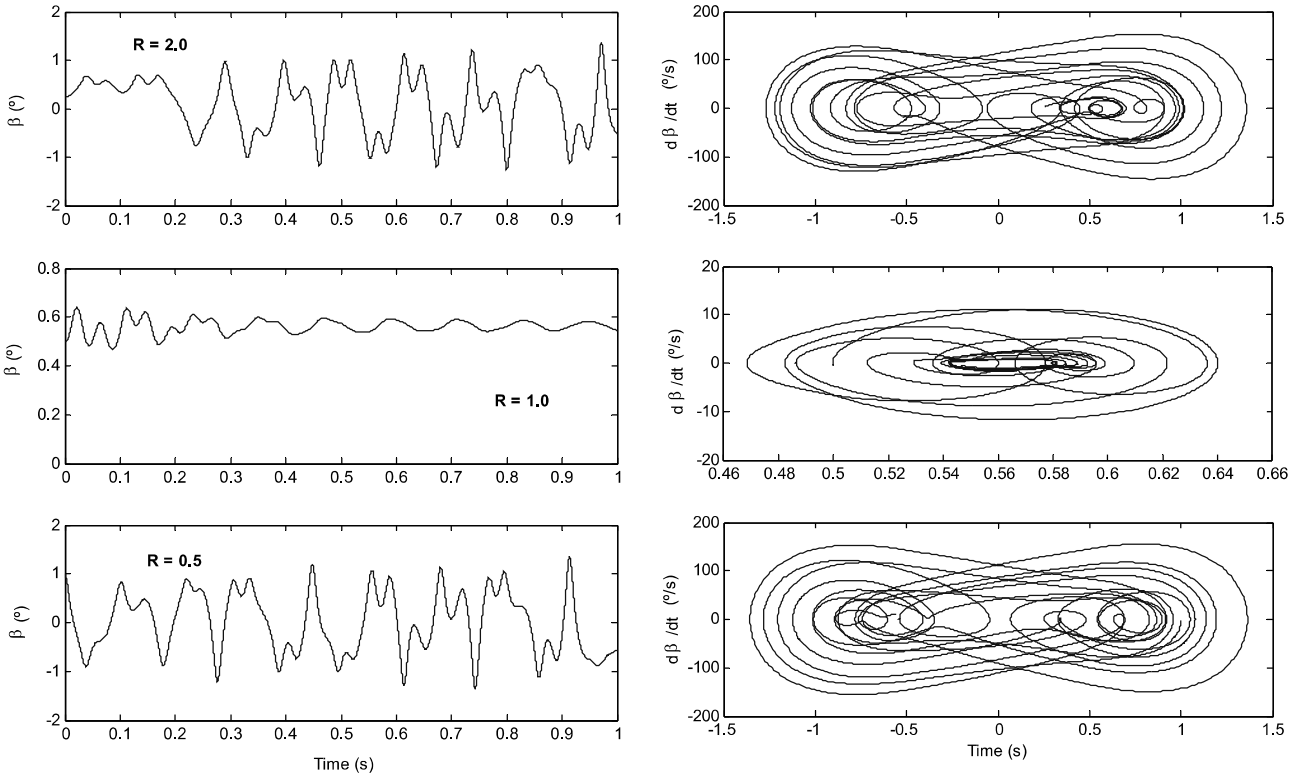

Figura 6. Time responses and phase trajectories of the non-linear model for various *R* and velocity of 45 m/s.

Figure 7 shows the time responses and phase trajectories of the non-linear case for the velocity of 75 m/s. For R = 2.0, 1.0 and 0.5 the typical LCO behavior is observed. The system response presents bounded motions consisting of a limited number of frequencies and amplitudes. This behavior is expected when a cubic hardening nonlinearity is considered. The linear behavior observed in the time response of Fig. 5 is clearly modified by the combined nonlinearity. The control surface is free inside the free-play gap, but its amplitude is limited by the cubic hardening stiffness.

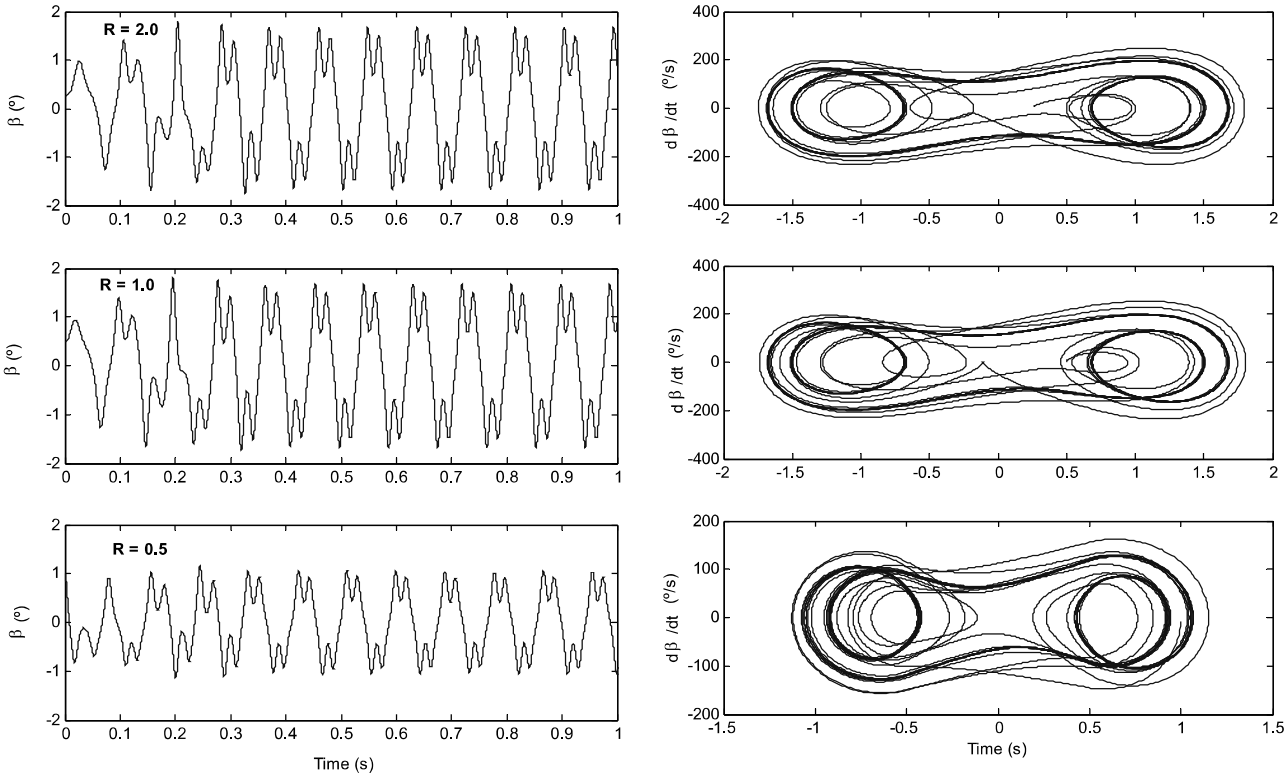

Figura 7. Time responses and phase trajectories of the non-linear model for various *R* and velocity of 75 m/s.

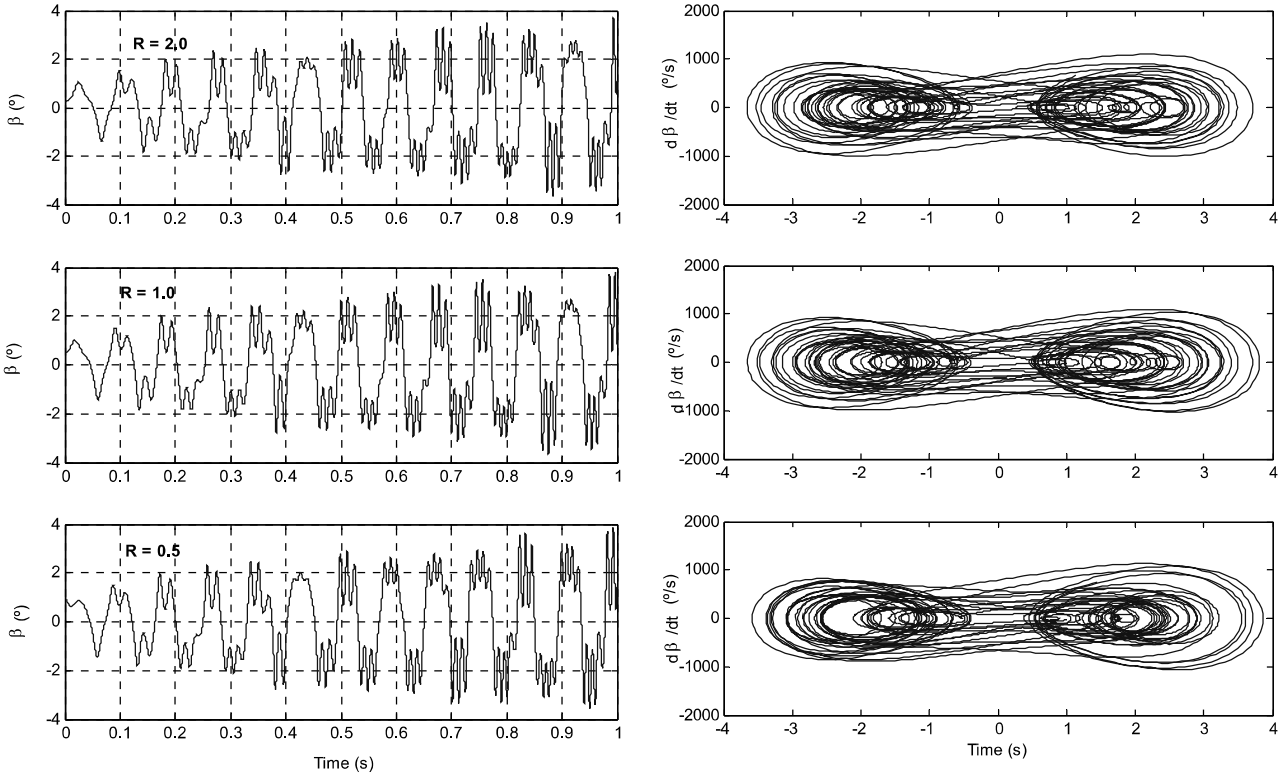

Figura 8. Time responses and phase trajectories of the non-linear model for various *R* and velocity of 85 m/s.

Figure 8 represents the time responses and phase trajectories of the non-linear case for the velocity of 85 m/s. For different values of *R* the system has a very similar behavior. The continual jump observed has a nonperiodic motion consisting of a multitude of frequencies and amplitudes, classified as the chaotic motion. In general, the time responses of Fig. 6 and 7 are bounded and the amplitudes of the signals are frequently limited to values quite similar to the free-play angle. This behavior is not verified in Fig. 8. In these cases, increasing amplitudes modified by the effect of the combined nonlinearity are observed.

CONCLUSIONS

This study dealt with a time domain aeroelastic model representing linear or non-linear three-degree-of-freedom typical section. The non-linear behavior is introduced considering a combined nonlinearity of free-play and cubic stiffening in the control surface degree-of-freedom. The system response is determined by time marching of the governing equations using a standard Runge-Kutta algorithm. The assumed nonlinearity has a smooth transition between the linear (free-play) and non-linear region (cubic), eliminating the problem to locate the ‘‘switching points’’ when free-play is considered, for example.

The non-linear analysis performed shows that responses are sensitive to the initial conditions, or to the ratio *R*. This is clear for velocities below the linear flutter one. In general, LCOs and chaotic motions are observed for any control surface initial conditions and velocities. The linear flutter behavior observed in Fig. 5 is converted into a chaotic motion when the non-linear analysis is done. The damped linear responses of Fig. 4 are converted into LCO motion when the non-linear analysis is performed. The short term damages of the linear flutter are converted into long term non-linear effects. Free-play gaps in aircraft flight control linkage systems are a concern from fatigue and inspection point of view.

REFERENCES

Bae, J.S., Inman, D.J. and Lee, I., 2004, “Effects of Structural Nonlinearity on Subsonic Aeroelastic Characteristics of an Aircraft Wing with Control Surface”, Journal of Fluids and Structures, Vol. 19, pp. 747, 763.

Brown, E.L., 2003, “Integrated Strain Actuation in Aircraft with Highly Flexible Composite Wings”, Phd Thesis, Massachusetts Institute of Technology.

Conner, M.D., Tang, D.M. and Dowell, E.H., 1997, “Nonlinear Behavior of a Typical Airfoil Section with Control Surface Freeplay”, Journal of Fluids and Structures, Vol.1, No. 1, pp. 89-109.

Dowell, E.H., 1995, “A Modern Course in Aeroelasticity”, Kluwer Academic Publishers, Netherlands, 699 p.

Katz, J. and Plotkin, A., 2001, “Low-Speed Aerodynamics”, Cambridge University Press, United Kingdom.

Lee, I. and Kim, S.H., 1995, “Aeroelastic Analysis of a Flexible Control Surface with Structural Nonlinearity”, Journal of Aircraft, Vol.32, No. 4, pp. 868-874.

Lee, M.J. and Hodges, D.H., 2004, “On the importance of aerodynamic and structural geometrical nonlinearities in aeroelastic behavior of high-aspect-ratio wings”, Journal of Fluids and Structures, Vol. 35, pp. 205, 334.

O’Neil, T., and Strganac, T.W., “Aeroelastic Response of a Rigid Wing Supported by Nonlinear Springs”, Journal of Aircraft, Vol. 35, No. 4, pp. 616, 622.

Patil, B.H.K., Price, S.J. and Wong, W.S., 1999, “Non-linear aeroelastic analysis of airfoils: bifurcation and chaos”, Progress in Aerospace Sciences, Vol. 19, pp. 905, 915.

Price, S.J., Lee, B.H.K. and Alighanbari , H., 1994, “Postinstability Behavior of a Two-Dimensional Airfoil with a Structural Nonlinearity”, Journal of Aircraft, Vol. 31, pp. 1395–1401.

Singh, S.N. and Yim,W., 2003, “State Feedback Control of an Aeroelastic System with Structural Nonlinearity”, Aerospace Science and Technology, N. 7, pp.23-31.

Tang, D. and Dowell, E.H., 2006, “Flutter and Limit-Cycle Oscillations for a Wing-Store Model with Freeplay”, Journal o Aircraft, Vol. 43, No. 2, pp. 487-503.

Tang, D.M. and Dowell, E.H., 1993, “Experimental and Theoretical Study for Nonlinear Aeroelastic Behaviour of a Flexible Rotor Blade”, AIAA Journal, Vol. 31, pp. 1133–1142.

Woolston, D.S., Runyan, H.L. and Andrews, R.E., 1957, “An Investigation of Effects of Certain Types of Structural Nonlinearities on Wing and Control Surface Flutter”, Journal of the Aeronautical Sciences, Vol. 24, pp. 57–63.

Zhang R. and Singh S.N., 2001, “Adaptive Output Feedback Control of an Aeroelastic System with Unstructured Uncertainties,” Jounal of Guidance, Control, and Dynamics, Vol. 24, N. 3, pp. 502-509.

Zhao, L.C. and Yang, Z.C., 1990, “Chaotic Motions of an Airfoil with Nonlinear Stiffness in Incompressible Flow”, Journal of Sound and Vibration, Vol.138, pp.245–254.

Zhao, Y.H. and Hu, H.Y., 2004, “Aeroelastic Analysis of a Non-Linear Airfoil Based on Unsteady Vortex Lattice Model,” Journal of Sound and Vibration, Vol. 276, pp. 491, 510.

RESPONSIBILITY NOTICE

The authors are the only responsible for the printed material included in this paper.